Berliner Hochschule für Technik

Fachbereich II
Mathematik - Physik - Chemie

01/2024

Diana Estévez Schwarz

Structured Second-Order Linear ODEs: Eigenvalues, Singular Values and the DMD

Strukturierte lineare Differentialgleichungen zweiter Ordnung: Eigenwerte, Singulärwerte und die DMD (englischsprachig)

Reports in Mathematics, Physics and Chemistry
Berichte aus der Mathematik, Physik und Chemie

ISSN (print): 2190-3913

Reports in Mathematics, Physics and Chemistry

Berichte aus der Mathematik, Physik und Chemie

The reports are freely available via the Internet:
https://www1.bht-berlin.de/FB_II/reports/welcome.htm

01/2024, August 2024

Structured Second-Order Linear ODEs: Eigenvalues, Singular Values and the DMD

Strukturierte lineare Differentialgleichungen zweiter Ordnung: Eigenwerte, Singulärwerte und die DMD (englischsprachig)

Editorial notice / Impressum

Published by / Herausgeber:
Fachbereich II
Berliner Hochschule für Technik
Luxemburger Str. 10
D-13353 Berlin
Internet: https://www.bht-berlin.de/ii

ISSN (print): 2190-3913

STRUCTURED SECOND-ORDER LINEAR ODES: EIGENVALUES, SINGULAR VALUES AND THE DMD

DIANA ESTÉVEZ SCHWARZ

Abstract. For certain classes of structured matrices, the eigenvalues can be estimated or even calculated explicitly by means of well-known formulas. Starting from these formulas, in this article we derive further formulas for the eigenvalues and singular values of structured matrices that result from second-order linear ODEs by order reduction. This insight leads to a better understanding of these relationships and permits the construction of large-scaled examples (or counterexamples) with specific characteristics that can be used for testing and teaching purposes. As applications, we discuss two well-known example classes, namely a simple discretized wave equation and simple spring-damper systems in series. On the one hand, we can recognize when complex eigenvalues appear and compute the stiffness index and stiffness ratio explicitly. On the other hand, if the dynamic mode decomposition (DMD) is applied to data generated with such ODEs, then the formulas allow to estimate the eigenvalues and singular values that are relevant in this context. For some of the mentioned examples we visualize and discuss the approximations obtained with the DMD with very low-dimensional dynamics.

1. Introduction

The theory of linear differential equations is well established and the importance of the eigenvalues well understood. Since many applications involve linear differential equations that have strong structural properties, eigenvalues of many structured matrices have been analyzed in detail and there exist very nice explicit formulas to compute them without numerical methods. However, for the matrices we get when we reduce the order of second-order ODEs, analogous formulas do not seem to be available yet, even if they are relatively easy to derive. For these matrices, in general the eigenvalues are not singular values and moreover, they may also be complex.

By deriving such formulas, we can better understand the properties of the solutions of the ODEs, especially stiffness. Moreover, with that knowledge of the ODEs, we can produce better understood data to test end verify data-driven methods for dynamical systems.

The dynamic mode decomposition (DMD) is a method developed for applications in fluid-dynamics to extract dynamic information from data and is based on a linear tangent approximation [17]. The method can be applied also to data resulting from other areas.

For someone with knowledge of differential equations it may be a good approach to understand how it works when applied to data generated as numerical solution of well-understood ODEs.

In this article, we describe the relationship of the above mentioned formulas for the eingenvalues of the ODEs and the eigenmodes of the DMD, especially with regard to the spectral radius of the iteration matrix.

Date: August 12, 2024.

Key words and phrases. differential equation, eigenvalues, singular values, block matrices, dynamic mode decomposition.

The results may particularly be interesting for instructors, since high-dimensional examples with well understood properties can be constructed easily. Moreover, by using results from the perturbation theory for eigenvalues [13], estimates for the order of magnitude of the spectrum of more general examples may be possible.

The article is organized as follows. The structured second order ODES that we consider are introduced in Section 2, where also the general formulas for eigenvalues and singular values are derived for the reduced first order ODEs.

In Section 3, the general formulas are applied to the ODE that results for the wave equation with the method of lines (MOL). Analogously, in Section 4, they are applied to simple spring-damper systems.

In Section 5, we briefly explain the first step of the DMD, that we analyze in detail for our purposes. Since our aim is to explore the relationship to numerically generated data, in Section 6 we discuss the formulas of the Euler method for ODEs in this context.

The transfer to estimations for the DMD are finally discussed in Section 7 and in Section 8 some illustrative numerical experiments are presented. A brief summary is given in Section 9 and in the Appendix 10 the needed results from linear algebra have been compiled.

2. Linear structured second order ODEs

We consider second order differential equations of the form

$$x'' = \alpha N x + \beta N x'$$

for a constant matrix $N \in \mathbb{R}^{n\times n}$ and factors $\alpha, \beta \in \mathbb{R}$. By order reduction, we obtain the first order differential equation

$$y' = \begin{pmatrix} 0 & I \\ \alpha N & \beta N \end{pmatrix} y, \quad \text{for} \quad y = \begin{pmatrix} x \\ x' \end{pmatrix},$$

where $I \in \mathbb{R}^{n\times n}$ stands for the identity matrix. In this section, we focus on the eigenvalues and singular values of the matrix

$$M = \begin{pmatrix} 0 & I \\ \alpha N & \beta N \end{pmatrix}$$

in dependence of the eigenvalues and singular values of the matrix N.

For completeness and latter considerations we remark that if N is invertible, then M is invertible as well and

$$M^{-1} = \begin{pmatrix} -\frac{\beta}{\alpha} I & \frac{1}{\alpha} N^{-1} \\ I & 0 \end{pmatrix}.$$

2.1. **Eigenvalues.** Considering the characteristic polynomial and using Theorem 10.1 from Appendix 10 as well as the Jordan normal form $N = R^{-1}JR$ we obtain

$$\begin{aligned}
\det(\lambda I - M) &= \det \begin{pmatrix} \lambda I & -I \\ -\alpha N & \lambda I - \beta N \end{pmatrix} \\
&= \det(\lambda I(\lambda I - \beta N) - \alpha N) \\
&= \det(\lambda^2 I - \lambda\beta N - \alpha N) \\
&= \det(\lambda^2 R^{-1}R - \lambda\beta R^{-1}JR) - \alpha R^{-1}JR) \\
&= \det(R^{-1}) \cdot \det(\lambda^2 I - \lambda\beta J - \alpha J) \cdot \det(R) \\
&= \det(\lambda^2 I - \lambda\beta J - \alpha J).
\end{aligned}$$

Therefore, if we assume that the eigenvalues of N are

$$\lambda_k^N, \quad k = 1, \ldots, n,$$

then the eigenvalues for M are pairwise

$$\begin{aligned}
\lambda_{2k-1}^M &= \frac{\beta\lambda_k^N}{2} + \sqrt{\left(\frac{\beta\lambda_k^N}{2}\right)^2 + \alpha\lambda_k^N}, \\
\lambda_{2k}^M &= \frac{\beta\lambda_k^N}{2} - \sqrt{\left(\frac{\beta\lambda_k^N}{2}\right)^2 + \alpha\lambda_k^N}.
\end{aligned}$$

Here we can perfectly appreciate the complex pairs of eigenvalues if the discriminant is negative, i.e. if

$$\alpha\lambda_k^N < -\left(\frac{\beta\lambda_k^N}{2}\right)^2.$$

Note that for $\lambda_k^N > 0$ this means

$$\alpha < -\beta^2\frac{\lambda_k^N}{4}.$$

Moreover, if there exists a λ_k^N such that

$$\alpha = -\beta^2\frac{\lambda_k^N}{4},$$

then M has a double eigenvalue $\lambda_{2k-1}^M = \lambda_{2k}^M$.

Remark 2.1. *Often the calculation of the real parts of the eigenvalues is important. Recall that if some eigenvalues of M have large negative real parts, then explicit integration schemes require very small step-sizes h_t for stability reasons, such that implicit A-stable integration schemes are much more appropriate. In these cases, the ODE $y' = My$ is stiff. Therefore, the formulas allow the characterization of the stiffness.*

2.2. **Singular values.** Let us suppose that

$$\sigma_k^N, \quad k = 1, \ldots, n$$

are the singular values of N and $N = U_N\Sigma_N V_N^T$ the singular value decomposition of N with $\Sigma_N = diag(\sigma_1^N, \ldots, \sigma_n^N)$, such that $NN^T = U_N\Sigma_N^2 U_N^T$, because the singular values of N are the roots of the eigen values of NN^T (and N^TN).

The singular values of the matrix M are the roots of the eigenvalues of

$$MM^T = \begin{pmatrix} 0 & I \\ \alpha N & \beta N \end{pmatrix}\begin{pmatrix} 0 & \alpha N^T \\ I & \beta N^T \end{pmatrix} = \begin{pmatrix} I & \beta N^T \\ \beta N & (\alpha^2+\beta^2)NN^T \end{pmatrix}$$

and

$$M^TM = \begin{pmatrix} 0 & \alpha N^T \\ I & \beta N^T \end{pmatrix}\begin{pmatrix} 0 & I \\ \alpha N & \beta N \end{pmatrix} = \begin{pmatrix} \alpha^2N^TN & \alpha\beta N^TN \\ \alpha\beta N^TN & I + \beta^2N^TN \end{pmatrix}$$

that coincide. For our purposes, we consider the characteristic polynomial of MM^T and Theorem 10.1 from Appendix 10

$$\begin{aligned}
\det(\lambda I - MM^T) &= \det\begin{pmatrix}(\lambda-1)I & -\beta N^T \\ -\beta N & \lambda I - (\alpha^2+\beta^2)NN^T\end{pmatrix} \\
&= \det((\lambda-1)I\left(\lambda I - (\alpha^2+\beta^2)NN^T\right) - \beta^2 NN^T) \\
&= \det(\lambda^2 I + \lambda\left(-(\alpha^2+\beta^2)NN^T - I\right) + \alpha^2 NN^T) \\
&= \det(U)\det(\lambda^2 I + \lambda\left(-(\alpha^2+\beta^2)\Sigma_N^2 - I\right) + \alpha^2\Sigma_N^2)\det(U^T) \\
&= \det(\lambda^2 I + \lambda\left(-(\alpha^2+\beta^2)\Sigma_N^2 - I\right) + \alpha^2\Sigma_N^2).
\end{aligned}$$

Therefore, for

$$\begin{aligned}
p_k &= -(\alpha^2+\beta^2)(\sigma_k^N)^2 - 1, \\
q_k &= \alpha^2(\sigma_k^N)^2,
\end{aligned}$$

we see that for the k-th quadratic equation the discriminant is

$$d_k = \left(\frac{(\alpha^2+\beta^2)(\sigma_k^N)^2+1}{2}\right)^2 - \alpha^2(\sigma_k^N)^2 \geq 0,$$

and the unsorted singular values $\hat{\sigma}_*^M$ of M can be calculated pairwise by

$$\begin{aligned}
\left(\hat{\sigma}_{2k-1}^M\right)^2 &= \frac{(\alpha^2+\beta^2)(\sigma_k^N)^2+1}{2} + \sqrt{d_k}, \\
\left(\hat{\sigma}_{2k}^M\right)^2 &= \frac{(\alpha^2+\beta^2)(\sigma_k^N)^2+1}{2} - \sqrt{d_k}.
\end{aligned}$$

Since, by construction,

$$-\frac{p_k}{2} = \frac{(\alpha^2+\beta^2)(\sigma_k^N)^2+1}{2} \geq \sqrt{\left(\frac{(\alpha^2+\beta^2)(\sigma_k^N)^2+1}{2}\right)^2 - \alpha^2(\sigma_k^N)^2} = \sqrt{d_k},$$

we can confirm $\left(\hat{\sigma}_k^M\right)^2 \geq 0$.

Observe that the order of the sorted singular values σ_k^M depends on α and β. Note further that, if N is symmetric and positive definite, the eigenvalues and singular values of N coincide, but the eigenvalues and singular values of M are different.

3. Wave equations

Let us consider the wave equation

$$u_{tt} = c^2\Delta u$$

with zero Dirichlet-Boundary conditions. To discretize with the method of lines (MOL) here we approximate the second derivatives of the right hand side with central differences. After reducing the order we obtain an ODE of the form

$$y' = \begin{pmatrix} 0 & I \\ -\frac{c^2}{h_x^2}N & 0 \end{pmatrix} y$$

i.e. $\alpha = -\frac{c^2}{{h_x}^2}$ and $\beta = 0$, while the matrix N depends on the dimension.

Note that these α, β imply

$$\lambda^M_{2k-1} = \frac{c}{h_x}\sqrt{-\lambda^N_k}, \tag{3.1}$$

$$\lambda^M_{2k} = -\frac{c}{h_x}\sqrt{-\lambda^N_k}, \tag{3.2}$$

for the eigenvalues and

$$d_k = \left(\frac{(\alpha\sigma^N_k)^2 - 1}{2}\right)^2$$

and

$$\hat{\sigma}_{2k-1} = \sqrt{\frac{(\alpha\sigma^N_k)^2+1}{2} + \frac{(\alpha\sigma^N_k)^2-1}{2}} = |\alpha|\,\sigma^N_k = \frac{c^2}{{h_x}^2}\sigma^N_k$$

$$\hat{\sigma_{2k}} = \sqrt{\frac{(\alpha\sigma^N_k)^2+1}{2} - \frac{(\alpha\sigma^N_k)^2-1}{2}} = 1$$

for the singular values.

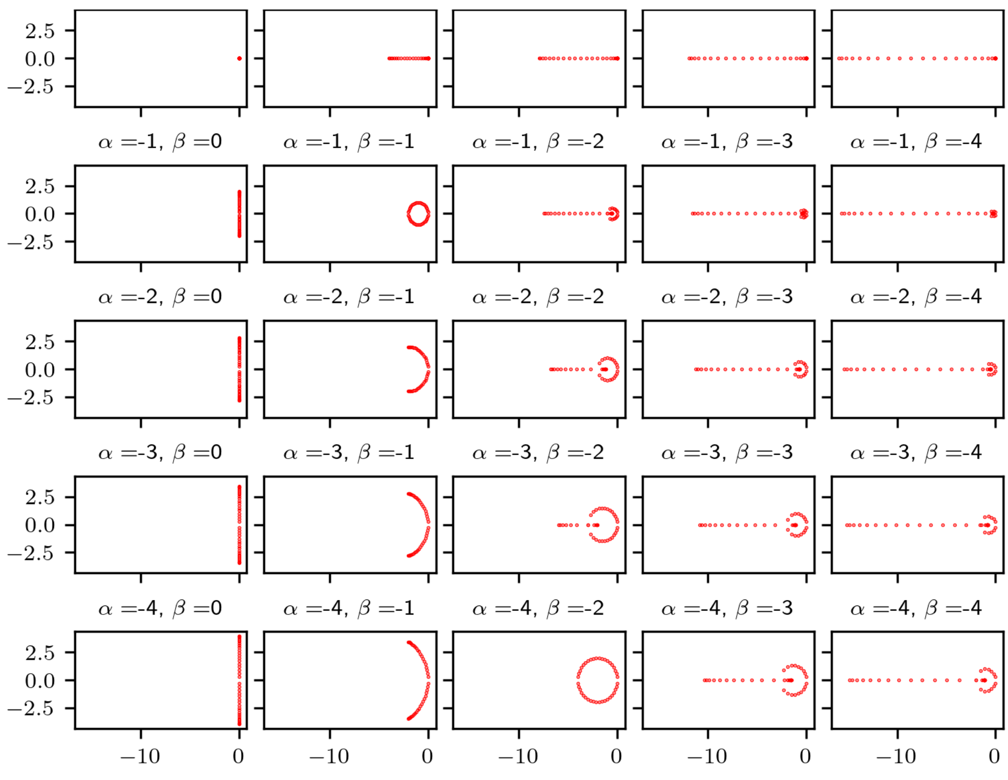

FIGURE 3.1. Eigenvalues of M for $N = N^{(1)}$ and different values of α and β. The red dots correspond to the complex eigenvalues in the plane.

3.1. **One-dimensional wave equation.** In the one-dimensional case, $N = N^{(1)}$ from the Appendix 10. Since $N^{(1)}$ is symmetric and positive definite, $0 < \sigma^N_k = \lambda^N_k < 4$, such

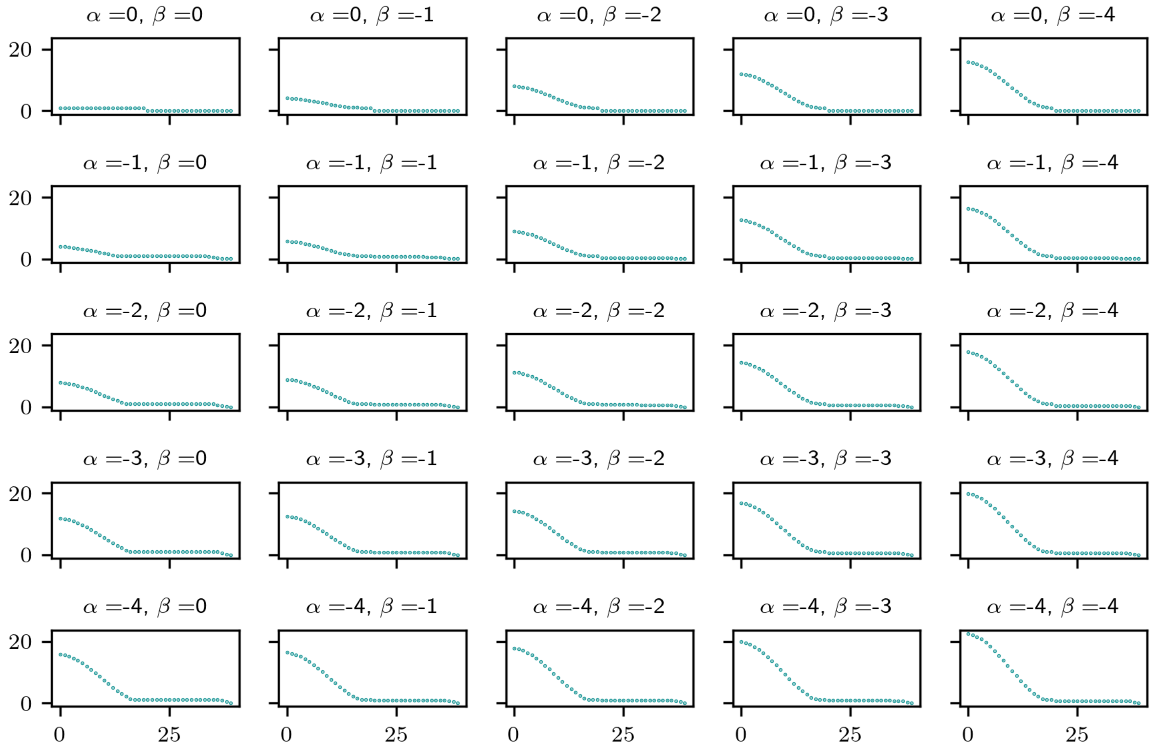

FIGURE 3.2. Singular values of M for $N = N^{(1)}$ and different values of α and β. Since singular values are real, the dots represent the decreasingly ordered values.

that

$$\begin{aligned} \lambda_{2k-1}^M &= \mathrm{i}\,\frac{c}{h_x}\sqrt{2-2\cos\left(\frac{k\pi}{n+1}\right)}, \\ \lambda_{2k}^M &= -\mathrm{i}\,\frac{c}{h_x}\sqrt{2-2\cos\left(\frac{k\pi}{n+1}\right)}, \end{aligned}$$

and therefore

$$\mathrm{Re}(\lambda_k^M) = 0, \quad -2\frac{c}{h_x} < \mathrm{Im}(\lambda_k^M) < 2\frac{c}{h_x}$$

as well as

$$\begin{aligned} \hat{\sigma}_{2k-1}^M &= \frac{c^2}{{h_x}^2}\left(2-2\cos\left(\frac{k\pi}{n+1}\right)\right), \\ \hat{\sigma}_{2k}^M &= 1 \end{aligned}$$

for $k = 1, \ldots, n$ and moreover

$$\mathrm{cond}\,(M) = \frac{\sigma_1^M}{\sigma_{2n}^M} = \frac{\max\left\{1, 2\frac{c^2}{{h_x}^2}\left(1-\cos(\frac{n\pi}{n+1})\right)\right\}}{\min\left\{1, 2\frac{c^2}{{h_x}^2}\left(1-\cos(\frac{1\pi}{n+1})\right)\right\}}.$$

Note that for $2\frac{c^2}{{h_x}^2}\left(1-\cos(\frac{\pi}{n+1})\right) < 1 < 2\frac{c^2}{{h_x}^2}\left(1-\cos(\frac{n\pi}{n+1})\right)$ we obtain $\mathrm{cond}\,(M) = \mathrm{cond}\,(N)$.

3.2. **Two-dimensional wave equation.** In the two-dimensional case, $N = N^{(4)}$ from the Appendix 10. Since $N^{(4)}$ is symmetric and positive definite, $0 < \sigma_k^N = \lambda_k^N < 8$, such that we obtain the unsorted values

$$\begin{aligned}
\hat{\lambda}_{j,2k-1}^M &= \mathrm{i}\,\frac{c}{h_x}\sqrt{4 - 2\cos\left(\frac{j\pi}{m+1}\right) - 2\cos\left(\frac{k\pi}{m+1}\right)}, \\
\hat{\lambda}_{j,2k}^M &= -\mathrm{i}\,\frac{c}{h_x}\sqrt{4 - 2\cos\left(\frac{j\pi}{m+1}\right) - 2\cos\left(\frac{k\pi}{m+1}\right)},
\end{aligned}$$

$$\mathrm{Re}(\hat{\lambda}_*^M) = 0, \quad -2\frac{c}{h_x} < \mathrm{Im}(\hat{\lambda}_*^M) < 2\frac{c}{h_x}$$

as well as

$$\begin{aligned}
\hat{\sigma}_{j,2k-1}^M &= \frac{c^2}{{h_x}^2}\left(4 - 2\cos\left(\frac{j\pi}{m+1}\right) - 2\cos\left(\frac{k\pi}{m+1}\right)\right) \\
\hat{\sigma}_{j,2k}^M &= 1
\end{aligned}$$

for $k = 1, \ldots, n$ and therefore

$$\mathrm{cond}\,(M) = \frac{\sigma_1^M}{\sigma_{2n}^M} = \frac{\max\left\{1, 4\frac{c^2}{{h_x}^2}\left(1 - \cos(\frac{n\pi}{n+1})\right)\right\}}{\min\left\{1, 4\frac{c^2}{{h_x}^2}\left(1 - \cos(\frac{1\pi}{n+1})\right)\right\}}.$$

3.3. **Conclusion for the wave equation.** Note that for very small h_x, the maximal absolute values of eigenvalues and the maximal singular values become huge.

4. Mass-spring-damper system in series

Let us consider n rigid bodies of equal mass m in series sliding in only one direction that are connected by equal linear spring-damper-systems with damping constant c and spring constant k.

In terms of Section 2, this means

$$\alpha = -\frac{k}{m}, \qquad \beta = -\frac{c}{m},$$

and matrices $N^{(1)}, N^{(2)}$ or $N^{(3)}$, depending on the attachment of the first and last bodies to rigid supports. Inserting the formulas from the Appendix 10 into the expressions of Section 2, explicit formulas result straight forward.

In Figures 3.1 and 3.2 the resulting eigenvalues and singular values are visualized for $N = N^{(1)}$ and different values of α and β.

4.1. **Consequences for stiffness.** Assuming that $\mathrm{Re}(\lambda_j) < 0$ holds for all eigenvalues, according to e.g. [14] the stiffness index is

$$L = \max_j |\mathrm{Re}\lambda_j|\,,$$

and the stiffness ratio

$$S = \frac{\max_j |\mathrm{Re}\lambda_j|}{\min_j |\mathrm{Re}\lambda_j|}.$$

With the above formulas, L and S may be computed explicitly.

Let us consider here $N^{(2)}$ and $\alpha < -\beta^2$, i.e. $km > c^2$, such that all eigenvalues are complex, and $\beta = -\frac{c}{m} < 0$, such that all eigenvalues have negative real part. Then it holds

$$\begin{aligned} L &= \beta\left(1-\cos\left(\frac{n\pi}{n+1}\right)\right) \leq 2\beta, \\ S &= \frac{\max_j |\mathrm{Re}\lambda_j|}{\min_j |\mathrm{Re}\lambda_j|} = \frac{\frac{\beta}{2}\left(2-2\cos\left(\frac{n\pi}{n+1}\right)\right)}{\frac{\beta}{2}\left(2-2\cos\left(\frac{1\pi}{n+1}\right)\right)} = \frac{1-\cos\left(\frac{n\pi}{n+1}\right)}{1-\cos\left(\frac{1\pi}{n+1}\right)}. \end{aligned}$$

Note that L increases with β, but S increases with n, independently of β.

5. First steps of the dynamic mode decomposition

The dynamic mode decomposition (DMD) is a numerical procedure for extracting dynamical features from data. Let us suppose that want to determine a the matrix M of an linear ODE

$$y' = My, \quad M \in \mathbb{R}^{n\times n}, n \in \mathbb{N}$$

from of a snapshot sequence

$$Y = \{y_1, y_2, \ldots, y_s\} \tag{5.1}$$

where $y(t_i) \approx y_i \in \mathbb{R}^n$ for equidistant $t_{i+1} = t_i + h$, $t_0, h \in \mathbb{R}$, $s \in \mathbb{N}$.

These snapshots are assumed to be related via a linear mapping described by a matrix A that remains approximately the same over the duration of the sampling period, i.e.

$$y_{i+1} \approx Ay_i$$

for $i = 1, \ldots s-1$. This implies that for

$$Y_{1,s-1} = \{y_1, y_2, \ldots, y_{s-1}\}, \quad Y_{2,s} = \{y_2, y_3 \ldots, y_s\}$$

we have a residual matrix R with

$$Y_{2,s} = AY_{1,s-1} + R,$$

such that $R \in \mathbb{R}^{n\times(s-1)}$ accounts for behaviors that cannot be described completely by the constant matrix A.

The output of the dynamic mode decomposition (DMD) is the eigenvalues and eigenvectors of the best-fit matrix A, which are referred to as the DMD eigenvalues and DMD modes respectively.

According to [2], the best-fit matrix A can be defined as

$$A_s = \min_A \|Y_{2,s} - AY_{1,s-1}\|_F = Y_{2,s}\left(Y_{1,s-1}\right)^+,$$

where $\|.\|_F$ is the Frobenius norm and $()^+$ denotes the pseudo-inverse, such that such that

$$y_{i+1} \approx A_s y_i.$$

The above approach corresponds to a forward DMD. Analogously, the backward DMD can be obtained interchanging Y_2, s and $Y_{1,s-1}$, cf. [4]. Therefore, in terms of a backward DMD we would compute a backward-time propagation matrix

$$B_s = \min_B \left\|BY_{2,s}^s - Y_{1,s-1}\right\|_F = Y_{1,s-1}\left(Y_{2,s}\right)^+,$$

such that

$$y_i \approx B_s y_{i+1}.$$

Here, we will not go into the details of the efficient computation of the (leading) eigenvalues of A_s or B_s, in particular for $n >> s$. Instead, we focus on the relationship between A_s, B_s and the matrix M.

6. Explicit and implicit Euler method

Solving the initial value problem

$$y' = My, \quad y(t_0) = y_0 \tag{6.1}$$

with the explicit Euler method with constant step-size h_t we obtain discrete solutions

$$y_{i+1} = (I + h_t M)\, y_i$$

such that for sufficiently small h_t

$$A \approx (I + h_t M) \quad \text{i.e.} \quad M \approx \frac{1}{h_t}(A - I) \tag{6.2}$$

can be assumed.

With the A-stable implicit (or backward) Euler method the discrete solutions are computed solving the linear systems

$$(I - h_t M)\, y_{i+1} = y_i$$

in each step. Therefore, for small h_t

$$B \approx (I - h_t M) \quad \text{i.e.} \quad M \approx \frac{1}{h_t}(I - B) \tag{6.3}$$

can be assumed.

Since stiff ODEs result in many applications, A-stable methods are often used, such that for the computation of the numerical solution in each time-step a system of equations has to be solved. Therefore, on the one hand the condition number of the corresponding matrix (that can be computed with the singular values) is of interest. On the other hand, if iterative solvers are used, then the eigenvalues are decisive for convergence. Indeed, the eigenvalues of large families of matrices M related to first-oder ODEs are well understood, motivated by their relevance for the solution of differential equations, s. Appendix 10.

For testing purposes, it seems likely to analyze well-understood ODEs $y' = My$ (6.1), to generate a snapshot sequence (5.1) with an established integration scheme, to determine then an approximation of M and to compare it to M itself.

As seen above, the spectrum of the matrix M can be approximated by the shifted and scaled DMD eigenvalues if the samples y_i have been generated numerically with Euler methods and an appropriate s is large enough.

Therefore, for small h_t and an appropriate s, we can assume that the DMD eigenvalues can be approximated with the help of the formulas below. For completeness, we include also the formulas for the singular values as well, since the largest singular value is crucial for the condition concept defined in [7].

Remark 6.1. *Note that for given A and B a better approximation of M may be achieved considering*

$$M \approx \frac{1}{2h_t}(A - B),$$

that reminds to the trapezoidal rule. However, with regard to the relationship between the eigenvalues of M and the DMD, we focus on A and the approximation (6.2).

7. Consequences for the DMD

Let us focus on the Euler method and suppose that h_t is sufficiently small and the estimations 6.2, 6.3 hold, i.e.

$$A \approx (I + h_t M) \quad \text{and} \quad B \approx (I - h_t M)\,.$$

If $\lambda_k^{(M)}$ are the eigenvalues of M, then the eigenvalues $\lambda_k^{(I+h_jM)}$ of $I + h_t M$ and $\lambda_k^{(I-h_jM)}$ of $I - h_t M$ result to be

$$\lambda_k^{(I+h_tM)} = 1 + h_t\lambda_k^{(M)}, \quad \lambda_k^{(I-h_tM)} = 1 - h_t\lambda_k^{(M)}.$$

Since in our approximations and in general M is not a normal matrix, we cannot assume that these eigenvalues are good approximations of the eigenvalues of A and B in general. But if all eigenvalues are different, then M is diagonalizable and estimations are possible, see also [3].

We will very briefly emphasize the following relationship between A and $I + h_t M$ (that coud be done analogously vor B and $I - h_t B$ going backward in time):

- According to Theorem 10.4, $y_{k+1} := Ay_k$ converges to zero iff $\rho(A) < 1$.
- Analogously, $y_{k+1} := (I + h_t M)y_k$ converges to zero iff $\rho(I + h_t M) < 1$.

For stiff ODEs, this means that the explicit (forward) Euler method becomes unstable if h_t is not small enough. Nevertheless, we can at least produce decaying numerical solutions choosing sufficiently small h_t. For the DMD, the influence of the step size is not so clearly visible, but may lead to the same instabilities.

Let us now focus on singular values. If $\sigma_k^{(M)}$ are the singular values of M, accordingly to Theorem 10.2 the singular values $\sigma_k^{(I+h_jM)}$ of $I + h_t M$ and $\sigma_k^{(I-h_jM)}$ of $I - h_t M$ can be estimated by

$$\sigma_k^{(I+h_tM)} \leq 1 + h_t\sigma_k^{(M)}, \quad \sigma_k^{(I-h_tM)} \leq 1 + h_t\sigma_k^{(M)}$$

and

$$\left|1 + h_t\lambda_1^{(M)}\right| \cdots |1 + \lambda_k M| = \left|\lambda_1^{(I+h_tM)}\right| \cdots |1 + \lambda_k I + h_t M| \leq \sigma_1^{(I+h_tM)} \cdots \sigma_k^{(I+h_tM)},$$
$$\left|1 - h_t\lambda_1^{(M)}\right| \cdots |1 - \lambda_k M| = \left|\lambda_1^{(I-h_tM)}\right| \cdots \left|1 + \lambda_k^{(I-h_tM)}\right| \leq \sigma_1^{(I-h_tM)} \cdots \sigma_k^{(I-h_tM)},$$

for $k = 1, \ldots, n-1$.

If we suppose that these approximations can be used to estimate the singular values of A and B, this result becomes relevant if we want to approximate exact A and B by lower-rank matrices A_k and B_k, see Theorem 10.3.

8. Numerical Tests

We discuss some tests for $N = N^{(1)} \in \mathbb{R}^{20\times 20}$ and correspondingly $M \in \mathbb{R}^{40\times 40}$. For the one-dimensional wave equation and $0 \leq x \leq 1$ this means $h_x = \frac{1}{19}$. For the numerical/iterative solutions we considered a time-step $h_t = 0.02/3$.

In a first approach, we computed a sequence $y_{n+1} = (I + h_t M)y_n$ and applied the DMD for small and large s. In this case, since the data were generated with a constant matrix $A = (I + h_t M)$, the results were as expected: larger s lead to better results in general.

Here, we focus on the results that we obtain when the numerical solutions of the ODE where computed with ivp-solve using the BDF-method. In this case, no constant matrix is given due to the time-step control, although the time-steps of the output are equidistant. As a consequence, only for small s reasonable results are obtained. For larger s, the computed approximations for eigenvalues and singular values are outside the expected range, leading to completely different results.

We visualize the solutions, eigenvalues and singular values for a better understanding. Observe that when the nonzero eigenvalues and/or singular values of A_s differ considerably from the range of those from $I + h_t M$, the numerical solutions are quickly drifting apart.

8.1. **Tests for $N^{(1)}$, $a = -15$, $b = 0$.** In this case, the exact solution is periodic. For the visualization, we interpret it as a one-dimensional wave equation and visualize the first components that correspond to u.

For $s = 1$ the matrix A_1 is constructed only with y_0 and y_1, and the nontrivial eigenvalue is almost 1, such that $y_{k+1} = A_1 y_k$ is almost constant, see Figure 8.3.

Computing $\rho(I + h_t M) = 1.0013250093925377$ and

$$\begin{aligned}
\rho(A_1) &= 0.9999133096993169, \quad \rho(A_2) = 0.9995785243278807, \\
\rho(A_3) &= 1.0083679570425916, \quad \rho(A_4) = 0.9996800991345408, \\
\rho(A_5) &= 1.1390517397969253, \quad \rho(A_6) = 1.7150384113562607,
\end{aligned}$$

the numerical diverging solutions for $s = 5, 6$ become plausible. Note also that for $s = 6$ the largest singular value is unexpectedly larger, see 8.5.

8.2. **Tests for $N^{(1)}$, $a = -10$, $b = -5$.** In this case, the exact solution is damped. For the visualization, we interpret it as a damped one-dimensional wave equation and visualize the first components that correspond to a damped u.

Again, for $s = 1$ the matrix A_1 is constructed only with y_0 and y_1, and the nontrivial eigenvalue is almost 1, such that $y_{k+1} = A_1 y_k$ is almost constant, see Figure 8.8.

In this case, $\rho(I + h_t M) < 1$ and $\rho(A_s) < 1$ for $s = 1, \dots, 6$. However, for large h_t also $\rho(I + h_t M) > 1$ become possible, such that $y_{k+1} = (I + h_t M) y_k$ diverges.

Note also that although $\rho(A_6) = 0.9988081280393623$, the corresponding solution in Figure 8.8 is undamped and the largest singular value is again unexpectedly larger, see 8.10.

9. Summary

It is well know that the analytical solution of $y' = My$ can be described with eigenvalues and eigenvectors of M. Here, we presented some formulas to derive the eigenvalues and singular values for specific matrices M that result from order reduction.

With the developed formulas we discerned the relationship between the eigenvalues and singular values of some matrices related to simple PDEs and spring-damper systems and the corresponding DMD. With this insight, we discussed these classes of examples and tested representative examples.

10. Appendix: Linear Algebra toolbox and results

10.1. Determinants of Block Matrices.

Theorem 10.1. *Consider $A, B, C, D \in \mathbb{R}^{n \times n}$, $n \in \mathbb{N}$ and block matrices*

$$M := \begin{pmatrix} A & B \\ C & D \end{pmatrix} \in \mathbb{R}^{2n \times 2n}. \tag{10.1}$$

(1) *If A is invertible, then*

$$\det(M) = \det(A)\det(D - CA^{-1}B).$$

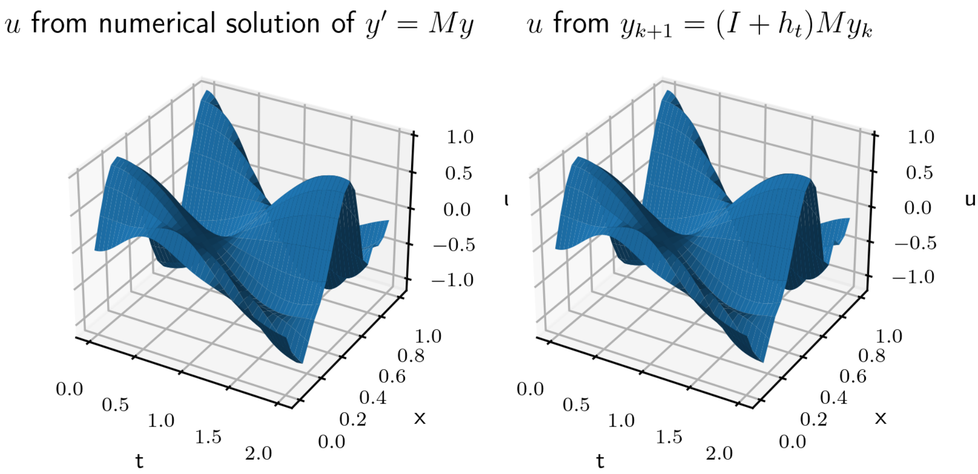

FIGURE 8.1. Numerical solutions for M with $N = N^{(1)}$ from the Appendix 10, and $a = -15$, $b = 0$ with solve-ivp (left) and the explicit Euler method (right).

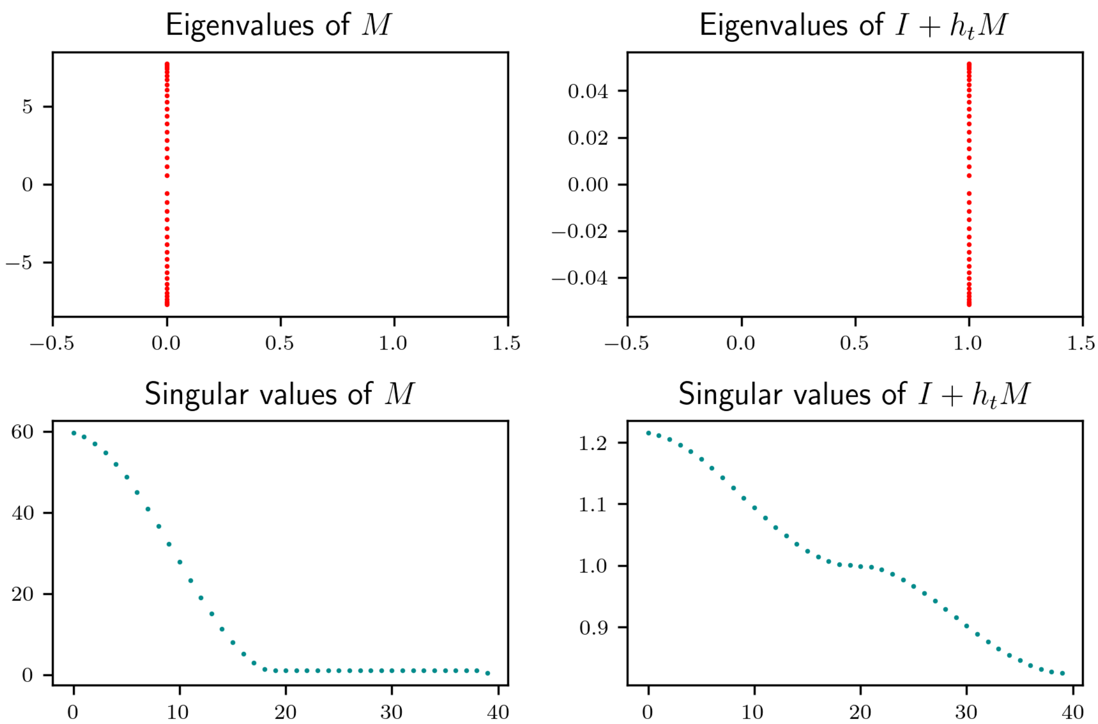

FIGURE 8.2. Eingenvalues and singular values for M with $N = N^{(1)}$ from the Appendix 10, and $a = -15$, $b = 0$. The eigenvalues are represented in the complex plane, the singular values sorted by indices.

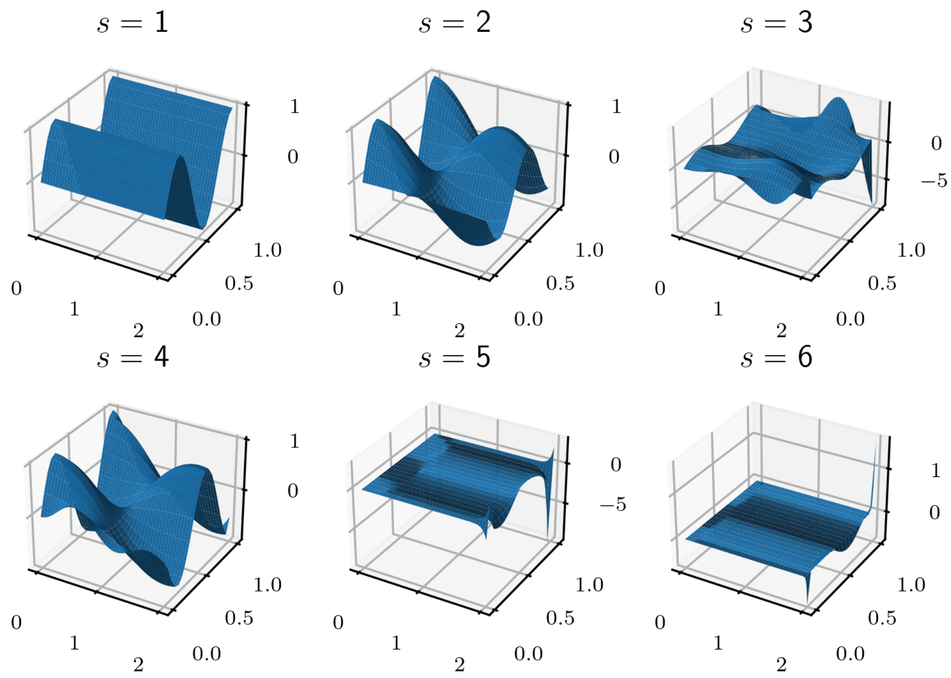

FIGURE 8.3. Solutions $y_{k+1} = A_s y_k$, where A_s for $s = 1, \ldots, 6$ was computed from the first steps of the solution visualized in Figure 8.1 on the left.

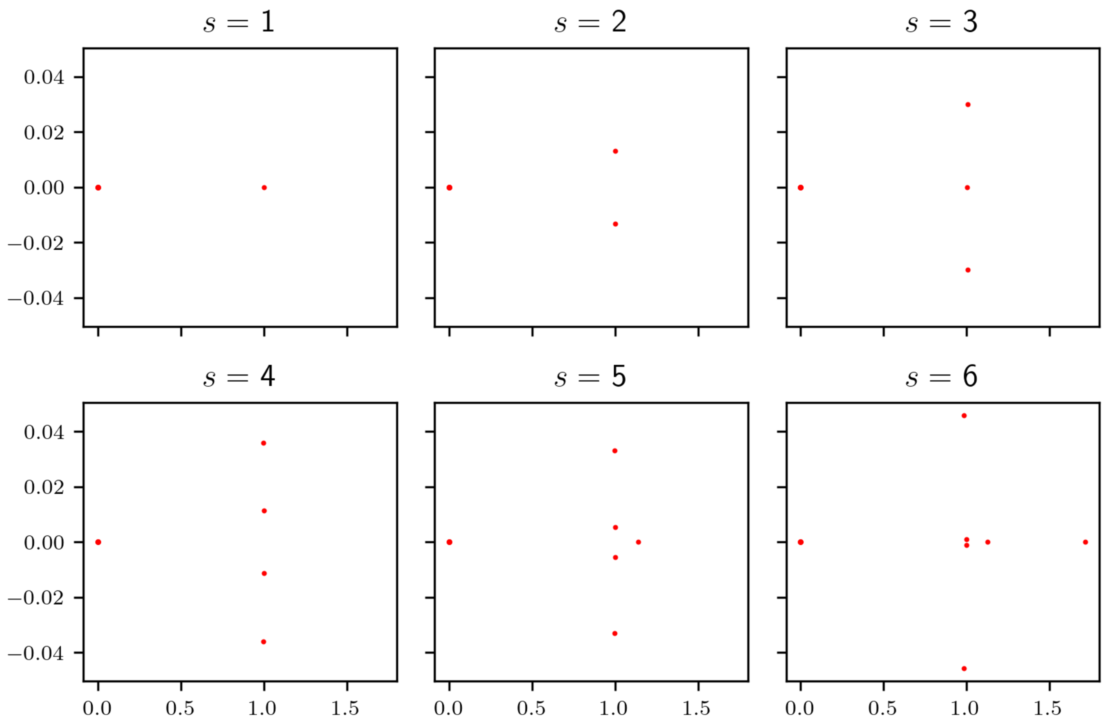

FIGURE 8.4. Eigenvalues of A_s in the complex plane, where A_s for $s = 1, \ldots, 6$ was computed from the first steps of the solution visualized in Figure 8.1 on the left.

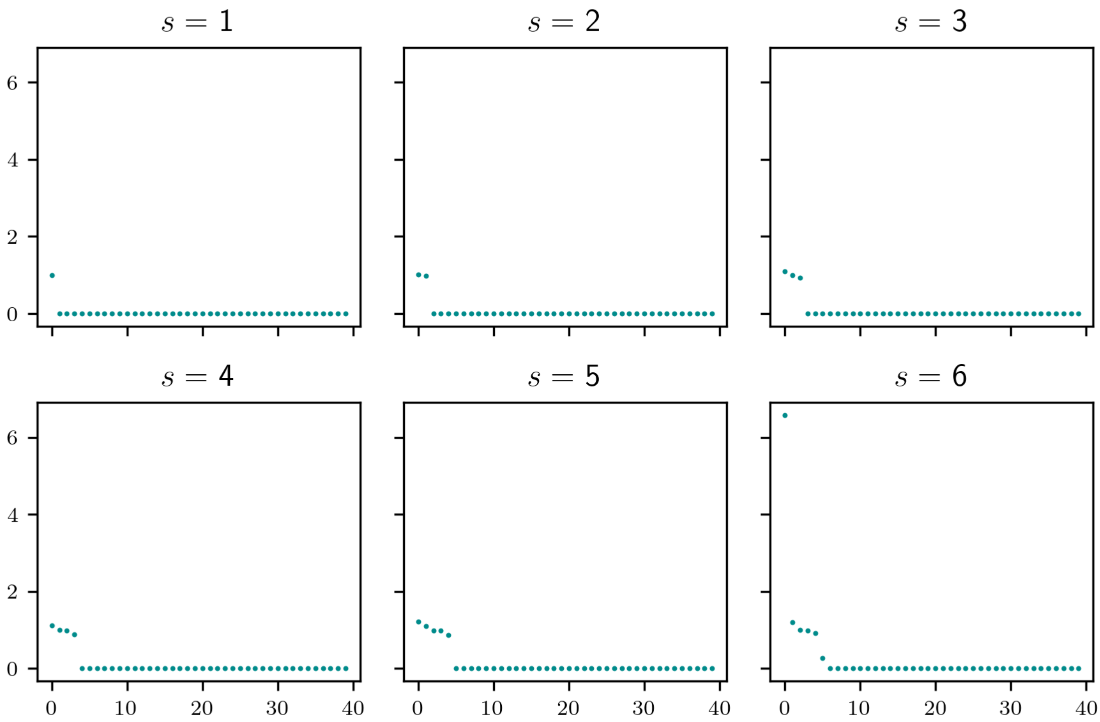

FIGURE 8.5. Decreasing singular values of A_s, where A_s for $s = 1, \ldots, 6$ was computed from the first steps of the solution visualized in Figure 8.1 on the left. Note that only s singular values are greater than zero.

(2) *If D is invertible, then*

$$\det(M) = \det(A - BD^{-1}C)\det(D).$$

(3) *If A is invertivle and $AC = CA$, or D is imvertible and $DC = CD$, then*

$$\det(M) = \det(AD - CB)$$

These formulas result from the factorizations

$$\begin{aligned} M &= \begin{pmatrix} 0 & 0 \\ CA^{-1} & I \end{pmatrix} \begin{pmatrix} A & 0 \\ 0 & D - CA^{-1}B \end{pmatrix} \begin{pmatrix} I & A^{-1}B \\ 0 & I \end{pmatrix}, \\ M &= \begin{pmatrix} I & BD^{-1} \\ 0 & I \end{pmatrix} \begin{pmatrix} A - BD^{-1}C & 0 \\ 0 & D \end{pmatrix} \begin{pmatrix} I & 0 \\ D^{-1}C & I \end{pmatrix}. \end{aligned}$$

10.2. **Formulas for Eigenvalues.** There is very extensive literature on the computation of eigenvalues of matrices with some structural properties, cf. [15], [9], [6], [16], [10] , among others. Here, we focus on tridiagonal and block tridiagonal matrices.

10.2.1. *Tridiagonal matrices.* It is well established that the eigenvalues of the matrix

$$N^{(1)} = \begin{pmatrix} 2 & -1 & & & \\ -1 & 2 & -1 & & \\ & -1 & \ddots & \ddots & \\ & & \ddots & \ddots & -1 \\ & & & -1 & 2 \end{pmatrix} \in \mathbb{R}^{n \times n}$$

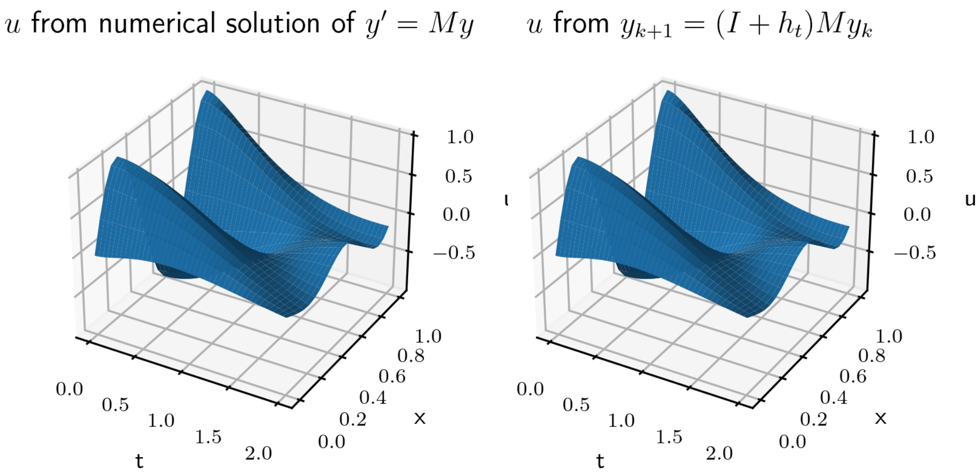

FIGURE 8.6. Numerical solutions for M with $N = N^{(1)}$ from the Appendix 10, and $a = -10$, $b = -5$ with solve-ivp (left) and the explicit Euler method (right).

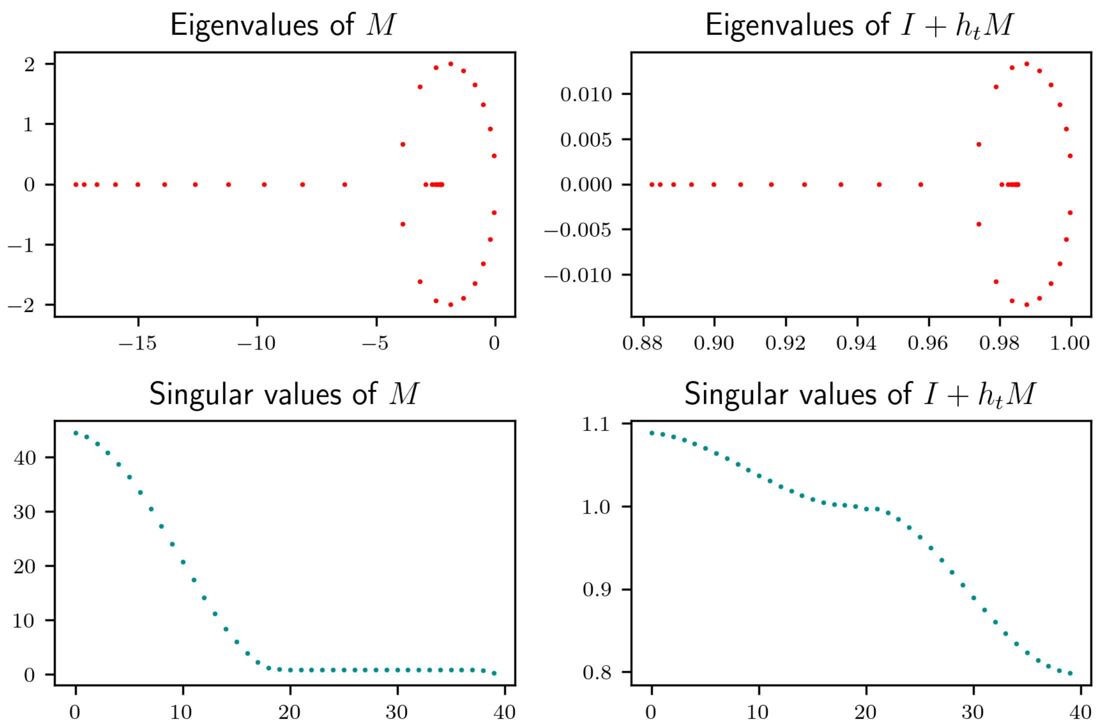

FIGURE 8.7. Eingenvalues and singular values for M with $N = N^{(1)}$ from the Appendix 10, and $a = -10$, $b = -5$. The eigenvalues are represented in the complex plane, the singular values sorted by indices.

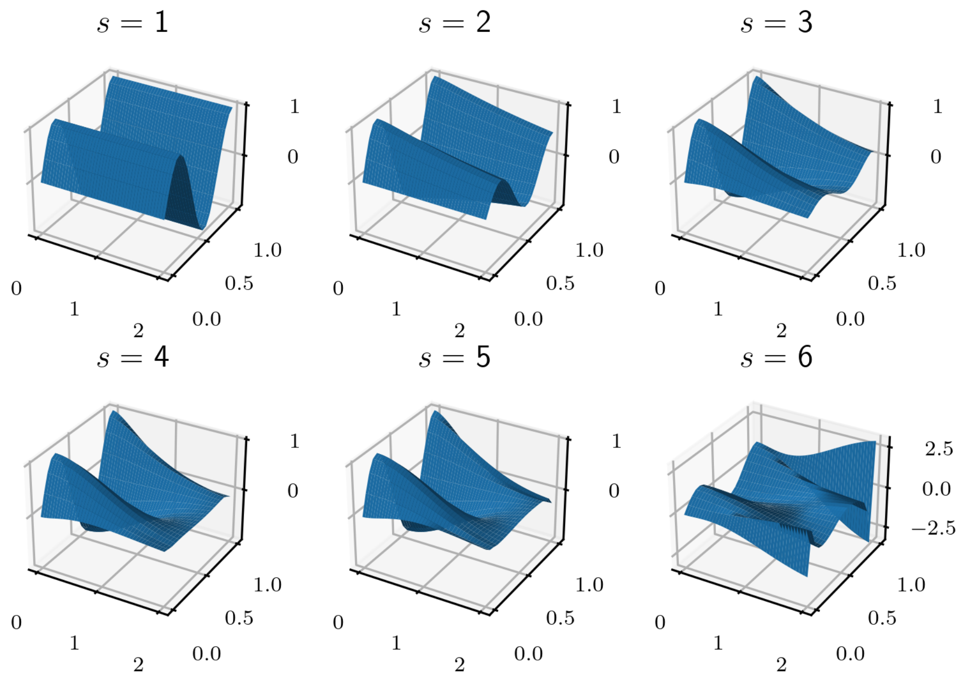

FIGURE 8.8. Solutions $y_{k+1} = A_s y_k$, where A_s for $s = 1, \ldots, 6$ was computed from the first steps of the solution visualized in Figure 8.6 on the left.

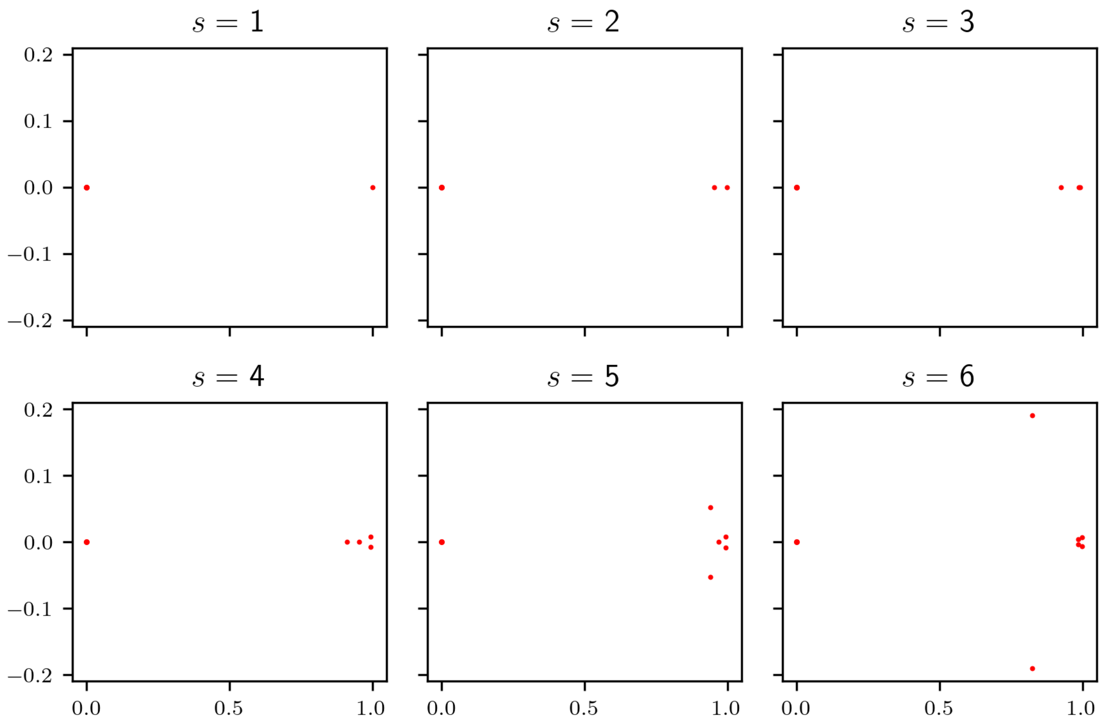

FIGURE 8.9. Eigenvalues of A_s in the complex plane, where A_s for $s = 1, \ldots, 6$ was computed from the first steps of the solution visualized in Figure 8.6 on the left.

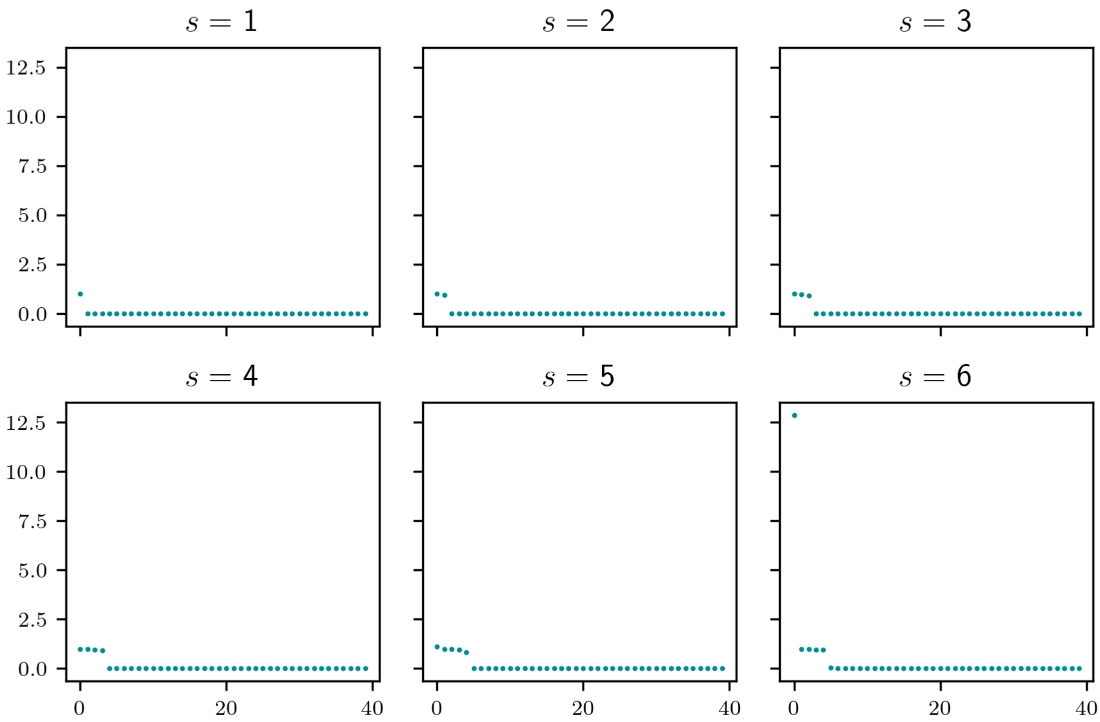

FIGURE 8.10. Decreasing singular values of A_s, where A_s for $s = 1, \ldots, 6$ was computed from the first steps of the solution visualized in Figure 8.6 on the left. Note that only s singular values are greater than zero.

are

$$\lambda_{k,n}^{(1)} = 2 - 2\cos\left(\frac{k\pi}{n+1}\right) , \qquad \text{for } k = 1, \ldots, n$$

while for the modified $(1,1)$ entry

$$N^{(2)} = \begin{pmatrix} 1 & -1 & & & \\ -1 & 2 & -1 & & \\ & -1 & \ddots & \ddots & \\ & & \ddots & 2 & -1 \\ & & & -1 & 2 \end{pmatrix} \in \mathbb{R}^{n \times n}$$

they result to be

$$\lambda_{k,n}^{(2)} = 2 - 2\cos\left(\frac{(2(k-1)+1)\pi}{2n+1}\right) , \qquad \text{for } k = 1, \ldots, n.$$

Moreover, if we consider the modified $(1,1)$ and (n,n)-entries

$$N^{(3)} = \begin{pmatrix} 1 & -1 & & & \\ -1 & 2 & \ddots & & \\ & \ddots & \ddots & -1 & \\ & & -1 & 2 & -1 \\ & & & -1 & 1 \end{pmatrix} \in \mathbb{R}^{n \times n}$$

we get

$$\lambda_{k,n}^{(3)} = 2 - 2\cos\left(\frac{(k-1)\,\pi}{n}\right), \qquad \text{for } k = 1, \dots, n.$$

More general formulas for tridiagonal matrices can be found in [5], [9], [11], [12] and the references therein. Here, we only want to note that in particular for $N^{(1)}$ the Matrix of eigenvectors is given by

$$V^{(1)} = \begin{pmatrix} \sin\left(\frac{\pi}{n+1}\right) & \dots & \sin\left(n\frac{\pi}{n+1}\right) \\ \vdots & & \vdots \\ \sin\left(n\frac{\pi}{n+1}\right) & \dots & \sin\left(n^2\frac{\pi}{n+1}\right) \end{pmatrix}$$

with $(V^{(1)})^T V^{(1)} = \frac{n+1}{2}$. This corresponds to the discrete sine transform.

10.2.2. *Block tridiagonal matrices.* On the other hand, for $m \in \mathbb{N}$,

$$T = \begin{pmatrix} 4 & -1 & 0 & \cdots & 0 \\ -1 & 4 & -1 & & \vdots \\ 0 & \ddots & \ddots & \ddots & 0 \\ \vdots & & \ddots & \ddots & -1 \\ 0 & \cdots & 0 & -1 & 4 \end{pmatrix} \in \mathbb{R}^{m\times m},$$

and the identity matrix $I_m \in \mathbb{R}^{m\times m}$ for $n = m^2$, the following matrix can be defined

$$N^{(4)} = \begin{pmatrix} T & -I_m & 0 & \cdots & 0 \\ -I_m & T & -I_m & & \vdots \\ 0 & \ddots & \ddots & \ddots & 0 \\ \vdots & & \ddots & \ddots & -I_m \\ 0 & \cdots & 0 & -I_m & T \end{pmatrix} \in \mathbb{R}^{n\times n}.$$

This matrix is a block Toeplitz symmetric tridiagonal matrix. For these matrices, there are also explicit formulas, s. [1] and the references therein. Indeed, the eigenvalues of this particular matrix read

$$\lambda_{j,k,n}^{(4)} = 4 - 2\cos\left(\frac{j\pi}{m+1}\right) - 2\cos\left(\frac{i\pi}{m+1}\right), \quad 1 \le i, j \le m$$

In particular we obtain the bounds

$$0 < \lambda_{k,n}^{(1)} < 4, \quad 0 < \lambda_{k,n}^{(2)} < 4, \quad 0 \le \lambda_{k,n}^{(3)} < 4, \quad 0 < \lambda_{j,k,n}^{(4)} < 8.$$

10.3. **Some inequalities.**

Theorem 10.2 (Weyl, [18])**.**

(1) *For matrices $A, B \in \mathbb{C}^{n\times n}$ it holds*

$$\sigma_{i+j-1}(A+B) \le \sigma_i(A) + \sigma_j(B), \quad 1 \le i, j \le n, \quad i+j \le n+1,$$

and, in particular,

$$\sigma_i(A+B) \le \sigma_i(A) + \sigma_1(B), \quad 1 \le i \le n. \tag{10.2}$$

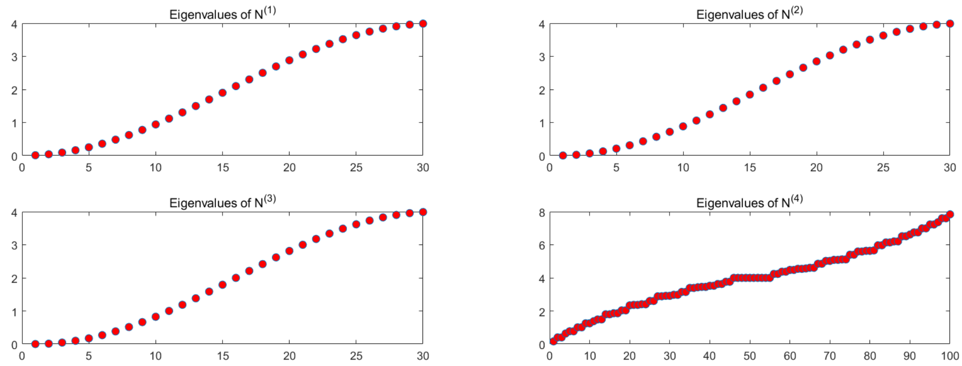

FIGURE 10.1. Eigenvalues (and singular values) of the symmetric matrices $N^{(1)}$, $N^{(2)}$, $N^{(3)}$ for $n = 30$ and $N^{(4)}$ for $m = 10$.

(2) *For any $A \in \mathbb{C}^{n\times n}$, if $\lambda_1, \dots, \lambda_n \in \mathbb{C}$ are the eigenvalues of A and the positive real numbers $\sigma_1, \dots, \sigma_n$ are the singular values of A, listed so that $|\lambda_1| \geq \cdots \geq |\lambda_n|$ and $\sigma_1 \geq \cdots \geq \sigma_n$, then*

$$|\lambda_1| \cdots |\lambda_n| = \sigma_1 \cdots \sigma_n \tag{10.3}$$

$$|\lambda_1| \cdots |\lambda_k| \leq \sigma_1 \cdots \sigma_k, \quad \textit{for } k = 1, \dots, n-1. \tag{10.4}$$

Theorem 10.3. *(Approximation Theorem [13])*
Let $A = U\Sigma V^T$ be the singular value decomposition of $A \in \mathbb{R}^{m\times n}$, with nonzero singular values $\sigma_1 \geq \sigma_2 \geq \dots \sigma_r > 0,$, $r = rank(A)$. For

$$k < r = \text{rank } (A)$$

and

$$A_k := \sum_{i=1}^{k} \sigma_i u_i v_i^T$$

it holds

$$\min_{\text{rank } (B)=k} \|A - B\|_2 = \|A - A_k\|_2 = \sigma_{k+1}.$$

This theorem means that there is no better rank-k approximation matrix B of A than the first k summands of the SVD.

For the DMD, this means that for all rank-s approximations M_s with $s < n$ it holds

$$\sigma_{s+1}^M \leq \|M - M_s\|_2 .$$

Lemma 10.4. *For $B \in \mathbb{R}^{n\times n}$ and $d \in \mathbb{R}^n$*

$$x^{(k+1)} := Bx^{(k)} + d$$

converges to a fixpoint for any starting point $x^{(0)}$ iff

$$\rho(B) < 1,$$

whereas $\rho(B)$ is the spectral radius of B

$$\rho(B) := \max\{|\lambda| : \lambda \textit{ is eigenvalue of } B\}.$$

References

[1] D. A. H. Ahmed: On the characteristic polynomial, eigenvalues for block tridiagonal matrices, Journal of Discrete Mathematical Sciences and Cryptography, volume, 25, nr. 5, pp- 1745-1756, 2022, Taylor & Francis. DOI: 10.1080/09720529.2020.1854939

[2] S. L. Brunton, J.N. Kurz, Data-Driven Science and Engineering: Machine Learning, Dynamical Systems, and Control, Cambridge University Press, 2019.

[3] Chen, Y., Peng, X. and Li, W. Relative perturbation bounds for eigenpairs of diagonalizable matrices. Bit Numer Math 58, 599–612 (2018). https://doi.org/10.1007/s10543-018-0701-5

[4] S. T. M. Dawson, M. S. Hemati, M: O. Williams, C. W. Rowley,Characterizing and correcting for the effect of sensor noise in the dynamic mode decomposition,Experiments in Fluids, Volumen 57, 2014.

[5] M. Elouafi, Eigenvalues and eigenvectors of tridiagonal matrices. Electronic Journal of Linear Algebra ISSN 1081-3810 A publication of the International Linear Algebra Society Volume 15, pp. 115-133, April 2006

[6] M. Elouafi, A.D. Aiat Hadj, On the characteristic polynomial, eigenvectors and determinant of a pentadiagonal matrix, Appl. Math. Comput. 198 (2008), 634-642.

[7] D. Estévez Schwarz, R. Lamour, A new projector based decoupling of linear DAEs for monitoring singularities, Numer Algor (2016) 73:535–565 DOI 10.1007/s11075-016-0107-x

[8] D. Estévez Schwarz and C. M. da Fonseca: On Singular Values Related to DAEs in Kronecker Canonical Form. Mediterranean Journal of Mathematics 13(5), pp. 2813-2826, (2016), DOI: 10.1007/s00009-015-0657-5.

[9] C. M. da Fonseca, On the eigenvalues of some tridiagonal matrices,J.Comput. Appl. Math.,200(2007), 283–286.

[10] C.M. da Fonseca, F. Yılmaz, Some comments on k-tridiagonal matrices: determinant, spectra, and inversion, Applied Mathematics and Computation Volume 270, 1 November 2015, 644-647.

[11] C. M. da Fonseca, V. Kowalenko, Eigenpairs of a family of tridiagonalmatrices: Three decades later,Acta Math. Hungar.,160(2020), 376–389.

[12] C. M. da Fonseca, V. Kowalenko, L. Losonczi, Ninety years of k-tridiagonal matrices, Stud. Sci. Math. Hung.,57(2020), 298–311.

[13] G.H. Golub, C. F. van Loan, Matrix Computations, Johns Hopkins University Press, 1996.

[14] Lawrence F. Shampine and Skip Thompson (2007), Scholarpedia, 2(3):2855. doi:10.4249/scholarpedia.2855

[15] L. Losonczi, Eigenvalues and eigenvectors of some tridiagonal matrices, Acta Math. Hung. 60 (1992), 309-322.

[16] T. McMillen, On the eigenvalues of double band matrices, Linear Algebra Appl. 431 (2009), 1890-1897.

[17] P. Schmidt, J. Sesterhenn, Dynamic Mode Decomposition of numerical and experimental data, Journal of Fluid Mechanics 656, November 2008, DOI:10.1017/S0022112010001217

[18] H. Weyl, Inequalities between the two kinds of eigenvalues of a linear transformation, Proc. Nat. Acad. Sci. U.S.A. 35 (1949), 408-411.

Berliner Hochschule für Technik, Luxemburger Str. 10, 13353 Berlin, Germany
Email address: estevez@bht-berlin.de